Journal of Pharmaceutical Analysis 15 (2025) 101070

Contents lists available at ScienceDirect

Journal of Pharmaceutical Analysis

journal homepage: www.elsevier.com/locate/jpa

Review paper

Advanced bioanalytical techniques for pharmacokinetic studies of nanocarrier drug delivery systems

Xiangjun Meng [a], Jiayi Yao [a], Jingkai Gu [b, c, *]

[a] School of Pharmaceutical Science and Technology, Faculty of Medicine, Tianjin University, Tianjin, 300072, China
[b] Research Center for Drug Metabolism, School of Life Sciences, Jilin University, Changchun, 130012, China
[c] State Key Laboratory of Supramolecular Structure and Materials, Center for Supramolecular Chemical Biology, College of Chemistry, Jilin University, Changchun, 130012, China

ARTICLE INFO

Article history:
Received 29 April 2024
Received in revised form
22 July 2024
Accepted 10 August 2024
Available online 14 August 2024

Keywords:
Nanocarrier drug delivery systems
Bioanalysis
Pharmacokinetics
Sample fractionation technique

ABSTRACT

Significant investment in nanocarrier drug delivery systems (Nano-DDSs) has yielded only a limited number of successfully marketed nanomedicines, highlighting a low rate of clinical translation. A primary contributing factor is the lack of foundational understanding of *in vivo* processes. Comprehensive knowledge of the pharmacokinetics of Nano-DDSs is essential for developing more efficacious nanomedicines and accurately evaluating their safety and associated risks. However, the complexity of Nano-DDSs has impeded thorough and systematic pharmacokinetic studies. Key components of pharmacokinetic investigations on Nano-DDSs include the analysis of the released drug, the encapsulated drug, and the nanomaterial, which present a higher level of complexity compared to traditional small-molecule drugs. Establishing an appropriate approach for monitoring the pharmacokinetics of Nano-DDSs is crucial for facilitating the clinical translation of nanomedicines. This review provides an overview of advanced bioanalytical methodologies employed in studying the pharmacokinetics of anticancer organic Nano-DDSs over the past five years. We hope that this review will enhance the understanding of the pharmacokinetics of Nano-DDSs and support the advancement of nanomedicines.

1. Introduction

The application of nanocarrier drug delivery systems (Nano-DDSs) in cancer diagnosis and treatment has been extensively explored. Despite continuous research efforts aimed at developing novel, enhanced, and sophisticated nanomedicines, their therapeutic potential remains largely unexploited. Clinically, only a limited number of nanoformulations have been successfully translated into new therapeutic agents. These include liposomal doxorubicin (Doxil/Caelyx [1,2] and Myocet [3]), liposomal daunorubicin (DaunoXome) [4], liposomal paclitaxel (Lipusu) [5], liposomal cytarabine (DepoCyt) [6], liposomal mifamurtide (Mepact) [7], liposomal vincristine (Marqibo) [8], liposomal irinotecan (Onivyde) [9], liposomal daunorubicin and cytarabine (Vyxeos) [10], albumin-bound paclitaxel (Abraxane) [11], paclitaxel micelle (Genexol-PM [12] and Apealea [10]), paclitaxel nanosuspension (PICN) [13], paclitaxel lipid nanoparticle (DHP107) [14], and Apealea (paclitaxel micellar) [14]. Despite these successes, the majority of nanomedicines failed during clinical trials. This challenge can be partly attributed to a limited understanding of the *in vivo* fate of Nano-DDSs. To improve the clinical translation success rate of nanomedicines, it is crucial to thoroughly understand their physicochemical properties, biocompatibility, pharmacokinetic, and pharmacodynamic behaviors. Such comprehensive understanding will enable researchers and clinicians to optimize the design and administration of nanomedicines, thereby improving their efficacy and safety in clinical applications.

In recent years, the majority of anti-cancer nanomedicine research has reported suboptimal tumor delivery efficiencies [15]. Furthermore, several nanomedicines that underwent clinical testing have been terminated due to safety concerns. For instance, in 2022, a single-arm phase II study combining NLG207, a nanoparticle camptothecin, with enzalutamide in advanced metastatic castration-resistant prostate cancer post-enzalutamide was terminated due to dose limiting toxicities [16]. The adverse effects may be attributed to the nanocarrier. In 2019, Merrimack ceased the development of MM-310, due to cumulative peripheral neuropathy detected in phase 1 trials [17].

* Corresponding author. Research Center for Drug Metabolism, School of Life Sciences, Jilin University, Changchun, 130012, China.
E-mail address: gujk@jlu.edu.cn (J. Gu).
Peer review under responsibility of Xi'an Jiaotong University.

https://doi.org/10.1016/j.jpha.2024.101070

Nanomedicines are designed to accumulate in tumors through enhanced permeability and retention (EPR) effect. Unlike healthy vessels, tumor vasculature is characterized by increased permeability and structural disorganization, featuring larger inter-endothelial gaps that facilitate the transendothelial migration of nanoparticles. This, coupled with the inefficient lymphatic drainage in tumors, impedes the clearance of extravasated nanoparticles, resulting in their accumulation within the tumor microenvironment. Upon entering the bloodstream, nanoparticles interact with plasma proteins, forming a protein corona that initiates opsonization [18,19]. This process marks the nanoparticles for rapid clearance by the mononuclear phagocyte system (MPS), particularly by macrophages [20]. Studies on the biodistribution of nanomaterials have demonstrated that a significant proportion of intravenously administered nanoparticles are sequestered in MPS organs such as the liver and spleen [19,20]. This nonspecific distribution can undermine pharmacological efficacy and raise potential safety concerns [21]. To mitigate these issues, surface modifications of nanoparticles, including the application of poly(ethylene glycol) (PEG), have been investigated to reduce opsonization [22]. However, repeated administration of PEGylated nanoparticles may induce the formation of PEG-specific antibodies, leading to accelerated blood clearance [23]. Therefore, to enhance the targeting capabilities of Nano-DDSs, a systematic evaluation and analysis of their *in vivo* fate is essential. Pharmacokinetic analysis plays a pivotal role in this process [24,25]. A comprehensive understanding of the pharmacokinetics of Nano-DDSs is imperative for the development of more efficacious nanomedicines and for the accurate assessment of their safety and risk [25–27].

Nano-DDSs can be broadly classified into two categories: organic and inorganic. Organic Nano-DDSs are further divided into polymer-based and lipid-based nanoparticles. Polymer-based nanoparticles include dendrimers, polymeric micelles, nanogels, nanospheres, polymeric nanoparticles, and polymer-drug conjugates, whereas lipid-based nanoparticles comprise liposomes, nanoemulsions, and solid lipid nanoparticles (SLNs) (Fig. 1). At present, the majority of nanomedicines approved for clinical use are organic Nano-DDSs formulated with either polymers or lipids [28–30]. These organic nanoparticles present significant challenges for *in vivo* analysis [31]. This review focuses on analytical methods specifically for organic Nano-DDSs. It provides a detailed overview of the latest advancements in bioanalytical techniques applied to pharmacokinetic studies of anticancer organic Nano-DDSs over the past five years. The aim of this review is to enhance the understanding of the pharmacokinetics associated with Nano-DDSs and to promote further development in the field of nanomedicine.

2. The research objectives of pharmacokinetic studies for organic Nano-DDSs

Nano-DDSs undergo a dynamic *in vivo* process, encompassing various forms such as drug-loaded nanoparticles, released drug, and dissociated nanocarrier materials. This process is intrinsically linked to their pharmacokinetic behavior, pharmacological effects, and toxicity profiles *in vivo*. Encapsulated drugs act as reservoirs, while the drug released at the target site, such as tumor tissue, forms the basis for therapeutic efficacy. To achieve the desired biological effect, it is crucial for the encapsulated drug to reach its designated target sites effectively and be released from the Nano-DDSs. Therefore, unlike conventional pharmacokinetic evaluations, measuring the total drug concentration alone in nanomedicine is insufficient to ascertain whether an efficacious concentration has been truly achieved within the tumor.

The interactions between the body and nanomaterials can potentially influence the pharmacokinetics, therapeutic efficacy, and safety of the encapsulated drug [32,33]. For example, PEG 2000 has been shown to inhibit the multidrug resistance related protein-2 (MRP2) [34]. Additionally, PEGs and their derivatives can inhibit the P-glycoprotein (P-gp)-mediated efflux system, thereby reducing P-gp activity and subsequently enhancing the absorption of its substrates [35,36]. Therefore, a comprehensive investigation of the pharmacokinetics of nanomaterials is crucial.

2.1. Released drug

The utilization of nanocarriers complicates the biodistribution and delivery of therapeutic drugs, presenting challenges in evaluating the efficacy of drug delivery [37]. Traditionally, the

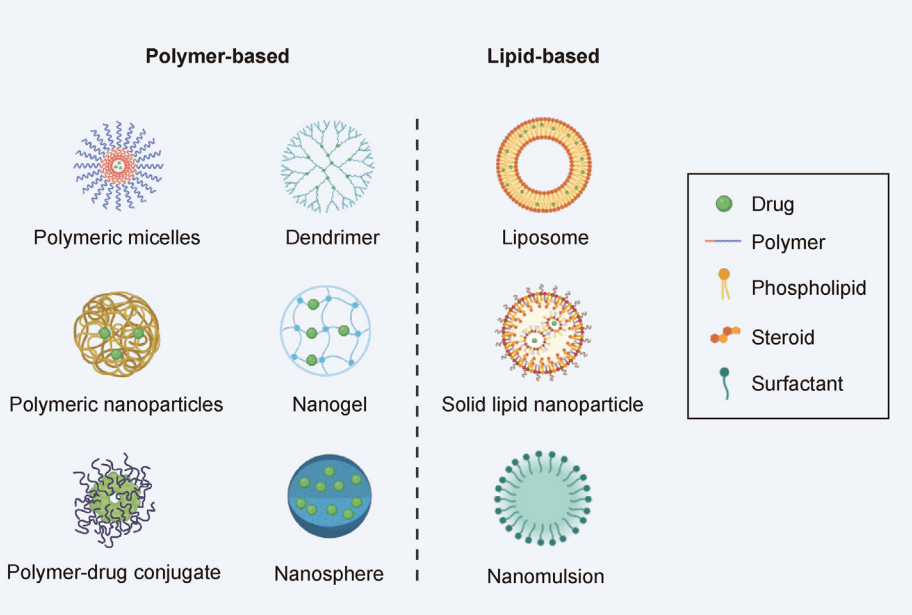

Fig. 1. Summary of the various categories of organic nanocarrier drug delivery systems (Nano-DDSs).

assessment of delivery efficacy has relied on proxies such as the accumulation of nanocarriers or the total drug within the tumor. However, these measurements do not fully capture the delivery of the active drug released at the target site. The effectiveness and safety of nanomedicine are contingent upon the concentration of the drug released in tumors and tissues, as only the released drug is available for therapeutic use. For example, in the case of doxorubicin liposomes, the therapeutic effect in tumor tissues is exerted by the released doxorubicin, while its presence in normal tissues and organs can lead to toxic side effects, such as cardiotoxicity [38].

2.2. Encapsulated drug

Encapsulated drugs act as inactive "prodrugs" until their release from nanocarriers [29,39]. Given that Nano-DDSs are designed to modify the pharmacokinetic profiles of encapsulated drugs for targeted therapy and enhanced therapeutic outcomes, a comprehensive evaluation and understanding of the absorption, distribution, metabolism, and excretion (ADME) processes of the drug in its encapsulated form are essential. This understanding is crucial for the design and customization of an optimal nanocarrier system [19,29], which is vital for clinical translation [31–33,40,41]. Failure to distinguish between encapsulated and released drugs will hinder the direct evaluation of the primary objective of drug encapsulation in nanoparticles, which is to facilitate drug delivery and release at the targeted site [37,42].

2.3. Nanomaterial

The preparation of Nano-DDSs necessitates the use of biocompatible nanomaterials that can be readily excreted from the body. The systematic preclinical development of these innovative nanomaterials requires tools to assess their pharmacokinetics, biodistribution, and elimination [43]. Unfortunately, the pharmacokinetics of nanomaterials is complex and challenging to predict [18,37,44–46]. For instance, commonly used polymeric nanomaterials exhibit a polydisperse nature in terms of molecular weight, with varying compositions and ratios of homologs, making their *in vivo* quantification extremely challenging [47,48]. To date, there remains a scarcity of advanced pharmacokinetic analysis on nanomaterials, particularly in the realm of organic nanomedicine [49,50], despite their prevalence in clinical trials and the market [31,51].

3. Analytical methods for pharmacokinetic studies of Nano-DDSs

Investigating the pharmacokinetics of Nano-DDSs requires a comprehensive understanding of the spatial and temporal trajectories of both the released and encapsulated drugs, as well as the nanomaterials involved (e.g., polymers, surfactants, and other auxiliary chemicals). A significant challenge in this field arises from the dynamic nature of drug release and carrier disintegration within biological environments [52]. Recent technological advancements have facilitated the development of novel methods for studying the pharmacokinetics of Nano-DDSs [53].

3.1. Radioisotope labeling

Radioisotope labeling is widely utilized to label drug molecules and polymer materials, facilitating the quantification of these substances based on the radioactive intensity detected in biological samples [54]. Various polymer-based nanomaterials, such as poly(lactic-co-glycolic) acid (PLGA) nanoparticles [55,56], poly lactic acid (PLA)-based nanoparticles [57], and others [58,59], have been radiolabeled with technetium-99m (^{99m}Tc). Reis et al. [60] investigated the tissue distribution of ^{99m}Tc-labeled PLA nanoparticles in mice, revealing that the majority of the nanoparticle formulations were taken up by the MPS. In a separate study, Rather et al. [61] investigated the pharmacokinetics and biodistribution of PLGA-based nanoparticles containing radiolabeled rifampicin in healthy human volunteers. Rifampicin was labeled with ^{99m}Tc using an indirect method. Single-photon emission computed tomography/computed tomography (SPECT/CT) imaging revealed the accumulation of nanoparticles in the distal regions of the intestine following the administration of the rifampicin nanoformulation. In a study conducted by Miedema et al. [62], a polyethylene glycol-b-pHPMAm-lactate block copolymer nanoparticle (CPC634) encapsulating docetaxel was labeled with zirconium-89 (^{89}Zr) for visualization and quantification via positron emission tomography/computed tomography (PET/CT) in seven patients with solid tumors. The application of a diagnostic dose of ^{89}Zr-CPC634 in PET/CT imaging facilitates the evaluation of tumor accumulation during treatment, offering potential for patient stratification in cancer nanomedicine that utilizes polymeric nanoparticles. Wang et al. [63] introduced a non-invasive method for *in vivo* tracking of the biodegradable polymer ε-poly-lysine (PLL) using radiolabeled fluorine-18 (^{18}F). Micro-PET imaging of radiolabeled F-PLLs demonstrated rapid clearance of these nanoparticles in the livers of rats. Given the significant potential of fluorinated polymers in gene and protein delivery, this straightforward ^{18}F radiolabeling approach for PET imaging is likely to be broadly applicable to a diverse range of fluorinated materials for monitoring their *in vivo* distribution. Nagachinta et al. [64] demonstrated a rapid and efficient radiolabeling technique utilizing facile-conjugated chemistry with ^{18}F for lipid-based nanocarriers. They conducted PET imaging and biodistribution studies in BALB/c mice to assess the pharmacokinetics of the radiolabeled nanometric emulsions and to determine their clearance pathways. In the study conducted by Wang et al. [65], tritium (^{3}H) was employed for quantitative pharmacokinetic analysis to elucidate the favorable pharmacokinetic profile of RNA nanoparticles. The radiolabeling of oligonucleotides was achieved through hydrogen-tritium exchange. This investigation involved collecting major organs from mice, including the brain, heart, lungs, liver, spleen, and kidneys, as well as tumors, to assess radiation biodistribution profiles via scintillation counting. The results indicated that approximately 5% of the ^{3}H-labeled RNA nanoparticles accumulated in tumors, with higher accumulation observed in tumors compared to the liver, heart, lungs, spleen, and brain following intravenous injection. Furthermore, the ^{3}H-labeled RNA nanoparticles exhibited rapid uptake in tumor vasculature within 30 min and sustained presence in tumors for over two days. Non-targeting ^{3}H-labeled RNA nanoparticles were detected in urine 30 min post-intravenous injection without undergoing degradation or processing. Over 55% of the intravenously administered radiolabeled RNA nanoparticles were eliminated from the body within 12 h, with the remaining 45% comprising radioactive counts that were unrecoverable due to whole-body distribution and blood dilution following intravenous administration. Dikpati et al. [43] employed a combination of radiolabeling and size exclusion chromatography, referred to as size exclusion of radioactive polymers (SERP), to investigate the distribution of ^{3}H radiolabeled trimethyl chitosan (TMC) in rats. Their study revealed the excretion of radiolabeled TMC nanoparticles in urine and feces over a 14-day period following administration to healthy rats, indicating efficient elimination of the polymer from the body. Pellico et al. [66] conducted a systematic review of current radiolabeling strategies for nanomaterials, providing a critical evaluation of their respective advantages and disadvantages. For further details, interested readers are encouraged to consult this review.

Radioisotope labeling is a well-established method renowned for its high sensitivity in tracking the distribution and clearance of nanocarriers. However, notable limitations are associated with radioisotope labeling, particularly the potential for detachment or leakage of radiolabels from nanocarriers. To address this challenge, methods such as radiochemical doping, physisorption, and cation exchange are under investigation. Despite these efforts, the metabolism of nanocarriers within the body can still lead to the detachment or leakage of labels. This issue is further complicated by the difficulty in distinguishing between signals from carrier-bound radiolabels and those from free or released radiolabels, as radiolabels from different sources can produce identical signals. Even if the radiolabels remain attached within the body, their impact on the *in vivo* behavior of nanocarriers must still be considered.

3.2. Stable isotope tracer ultrafiltration assay

In ultrafiltration, a significant concern is the impact of protein-bound drug components on the accurate quantification of both encapsulated and released drugs [67]. The Stern group has improved traditional ultrafiltration methodologies by incorporating a stable isotope tracer into plasma samples containing nanomedicine, thus enabling a more accurate assessment of plasma protein binding [68]. This innovative approach effectively addresses the key obstacle of differentiating the pharmacokinetic behaviors of different drug fractions in plasma. The stable isotope tracer ultrafiltration assay (SITUA) technique employs a trace amount of isotopically labeled drug (Fig. 2), under the assumption that the isotopically labeled drug will exhibit identical plasma protein binding behavior to that of the drug released from the nanomedicine. Specially, the isotopically labeled drug (D^*) is added into the nanomedicine-containing plasma and rapidly reaches binding equilibrium with plasma proteins. The plasma sample is subsequently transferred to an ultrafiltration device and separated by centrifugation. The total concentration of D^* in the plasma sample [Total D^*], the concentration of D^* in the ultrafiltrate [Ultrafiltrate D^*], the total concentration of the non-isotopically labeled drug (D) in the plasma sample [Total D], and the concentration of D in the ultrafiltrate [Ultrafiltrate D] are measured, respectively. The protein binding percentage of D^* (%Bound) is calculated by using Eq. (1) in Fig. 2. Since D^* exhibits identical protein binding characteristics to D, the protein binding percentage of D equals to that of D^*. Eq. (2) in Fig. 2 is used to determine the concentration of the unencapsulated drug [Unencapsulated D]. With %Bound and [Unencapsulated D] determined, the concentration of protein-bound D [Protein-bound D] can be determined using Eq. (3) in Fig. 2, and concentration of the concentration of the encapsulated drug [Encapsulated D] can be determined using Eq. (4) in Fig. 2.

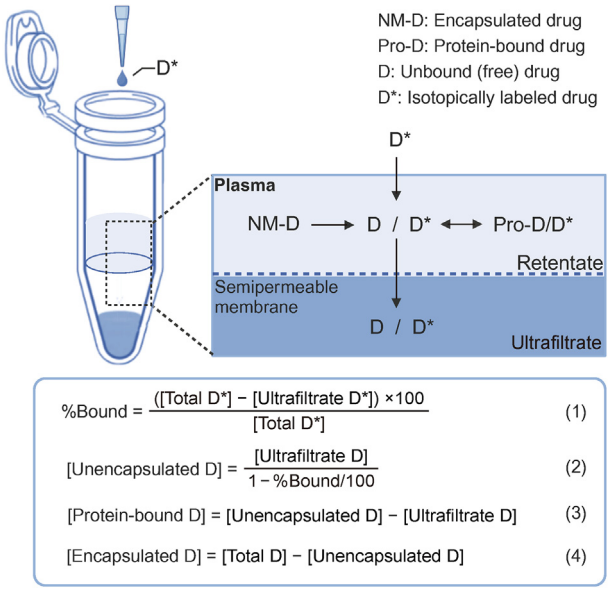

Fig. 2. Schematic illustration of the stable isotope tracer ultrafiltration assay (SITUA) technique.

The SITUA technique was employed to assess the pharmacokinetic profiles of Abraxane®, an FDA-approved nanomedicine containing paclitaxel, and its polymeric micelle formulation, Genexol®PM, for bioequivalence evaluation in the Sprague-Dawley rat model [69]. The findings revealed that, although Abraxane® and Genexol®PM exhibited nearly identical concentration-time profiles for total, released, and unbound drug fractions, statistically significant differences were observed in the pharmacokinetic parameters of the unencapsulated and unbound drugs between the two formulations. This discrepancy was not apparent in the total drug pharmacokinetic profile [69]. These results underscore the enhanced sensitivity of the SITUA approach in detecting subtle deviations from bioequivalence that may not be discernible using traditional methods focused solely on total drug pharmacokinetics [70].

The SITUA technique can provide concentration information for the encapsulated drug, unencapsulated protein-bound drug, and unencapsulated free drug in plasma samples. However, it is based on the assumption that the protein-binding behavior of the isotopically labeled drug in plasma will be identical to that of the released drug from nanomedicine. In reality, the concentration range of the released drug in plasma is wide, and the protein-binding percentage may vary at different concentrations, leading to potential inaccuracies. Therefore, it is necessary to verify that the plasma protein-binding percentages of the drug at different concentrations are consistent before using this method. Additionally, non-specific adsorption by the ultrafiltration device is also a concern.

3.3. Fluorescence imaging

Fluorescence imaging has been extensively employed to monitor the *in vivo* behavior of Nano-DDSs. Nanoparticles can be either internally loaded with fluorescent dyes or externally labeled on their surfaces with these dyes [71,72]. The quantification of nanoparticle uptake or biodistribution can be achieved by monitoring the fluorescence signal both *in vitro* and *in vivo*. It is generally assumed that the fluorescence signal emitted by nanoparticles is directly proportional to their accumulation within cells, tissues, or organs [73]. However, most traditional fluorophores do not exhibit environmental responsiveness, emitting consistent signals regardless of their attachment to a nanocarrier. Consequently, the observed signals represent a mixture of those from both nanocarrier-loaded and free probes, potentially compromising the precision of fluorescence imaging [74,75]. Recently, there has been significant focus on environment-responsive fluorescent probes that utilize the principles of Förster resonance energy transfer (FRET) [76–78], aggregation-caused quenching (ACQ) [79,80], and aggregation-induced emission (AIE) [81–83] (Fig. 3). These probes demonstrate simultaneous changes in fluorescence spectra in response to the dynamic alterations of nanocarriers [54].

3.3.1. FRET

FRET is a phenomenon wherein energy is transferred between two fluorophores, termed the donor and the acceptor, when they

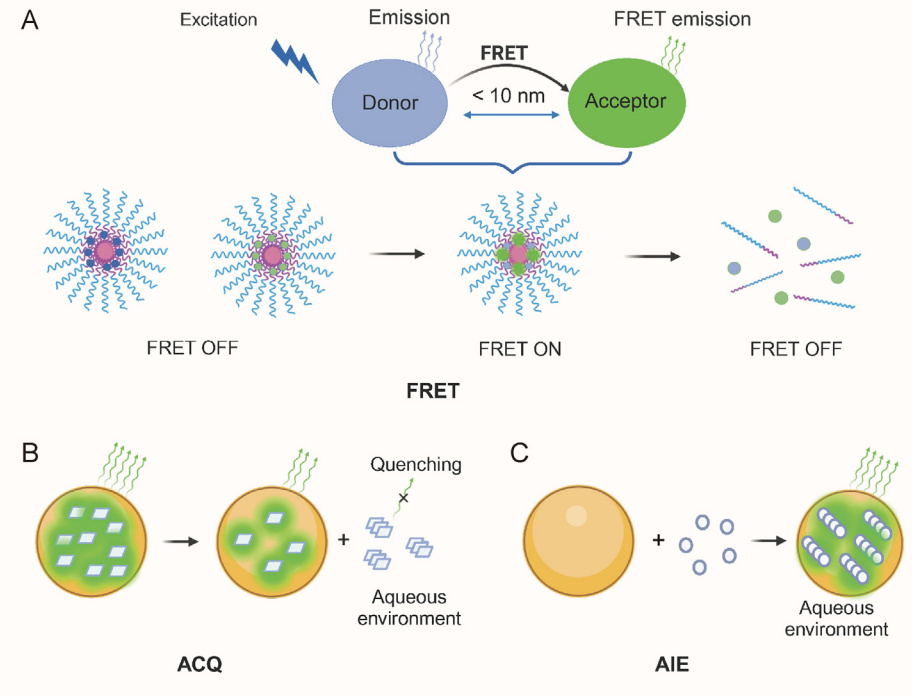

Fig. 3. Schematic representations of (A) Förster resonance energy transfer (FRET), (B) aggregation-caused quenching (ACQ), and (C) aggregation-induced emission (AIE).

are in an excited state. The efficiency of this energy transfer is inversely related to the distance between the two fluorophores, limiting the range of energy transfer to 1–10 nm (Fig. 3A) [84]. Donor and acceptor dyes can be loaded into nanocarriers to facilitate FRET, provided that the nanocarrier remains intact [73,85]. FRET offers the advantage of utilizing commonly used carbocyanine dyes, thereby facilitating the upgrade of existing fluorescence imaging techniques to incorporate FRET [31,86]. Consequently, FRET serves as a valuable tool for monitoring Nano-DDSs, including the assessment of nanoparticle integrity, drug release, and nanoparticle degradation. These parameters are crucial for gaining a fundamental understanding of the *in vitro* and *in vivo* behavior of nanoparticles, thereby providing essential information for optimizing their drug delivery applications [73,87].

Lebreton et al. [85] conducted a study on the pharmacokinetics of intact lipid nanocapsules (LNCs) following their intravenous administration in rats, with a subsequent reinjection after a 7-day interval, using FRET method for quantification. They developed a method to extract intact LNCs from blood via ultracentrifugation, which enhanced the efficiency of FRET signal. Quantification of intact LNCs was achieved through a combination of the FRET signal and nano tracker analysis. Pharmacokinetic data were analyzed using non-compartmental analysis and were utilized to construct a population pharmacokinetic model. Zhu et al. [88] employed FRET to investigate the *in vivo* distribution of a docetaxel-loaded, vitamin E-based, strongly reductive nanosystem (DTX-VNS) in BALB/c mice post-administration. The results indicated that the DTX-VNS nanosystem preferentially and rapidly releases the drug at tumor sites, as opposed to normal organs, due to the elevated levels of reactive oxygen species (ROS) present within the tumors. Sun et al. [89] conducted a study using the FRET principle, wherein a Cy5-modified survivin siRNA conjugated to nanogolds (Au-DR-siRNA) was encapsulated within lipid nanoparticles (LNPs) to observe *in vivo* siRNA release behavior. The findings indicated that upon the release of Au-DR-siRNA from the LNPs and its subsequent cleavage by the Dicer enzyme, free siRNA was generated within cells. This process caused the fluorescence of Cy5 to transition from a quenched state to an activated state, thereby indicating the location and timing of the siRNA release. Utilizing FRET to examine the kinetic stability of self-assembled poly(2-oxazoline) (POx) nanoparticles incorporating curcumin, Datta et al. [90] demonstrated a correlation between nanoparticle integrity and cellular uptake in human glioblastoma cells.

Based on FRET, Wang's group has developed a series of innovative designs to distinguish the localization of nanoparticles within and outside of cells [91,92]. Yin et al. [91] introduced a binary ratiometric nanoreporter (BiRN) that effectively differentiates intracellular from extracellular nanoparticle locations, thereby enabling quantitative imaging of nanoparticle internalization *in vivo* (Fig. 4). An acidic early endosomal pH (pH_{ee} ~6.0) was selected to monitor nanoparticle internalization events, as early endosome formation occurs rapidly following endocytosis. The 'OFF–ON' module remains 'OFF' in the tumor bloodstream and extracellular space (pH_e ~ 6.6–6.9), but switches 'ON' upon a rapid decrease in pH within the early endosome post-endocytosis. The 'always-ON' module serves as an internal standard for ratiometric quantitation of nanoparticle internalization. Following binary ratiometric processing, nanoparticles in the tumor microvasculature and extracellular space were excluded, facilitating real-time assessment of cellular internalization in live mice. Utilizing BiRN technology, the researchers effectively quantified the internalization of nanoparticles that accumulated in solid tumors across various levels of analysis, including whole-animal, intravital, excised tissue, and tissue section assessments.

Yan et al. [92] developed a pH/light dual-responsive monochromatic ratiometric imaging nanoparticle (MRIN) capable of selectively activating intracellular and extracellular fluorescence signals in response to acidic endocytic pH and near-infrared light (Fig. 5). This nanoparticle is labeled with a near-infrared fluorophore (Cy5) and a fluorescence quencher (Cy7.5), utilizing FRET to suppress fluorescence signals in the bloodstream and extracellular tumor space (pH_e ~ 6.7–7.1). Upon cellular internalization in

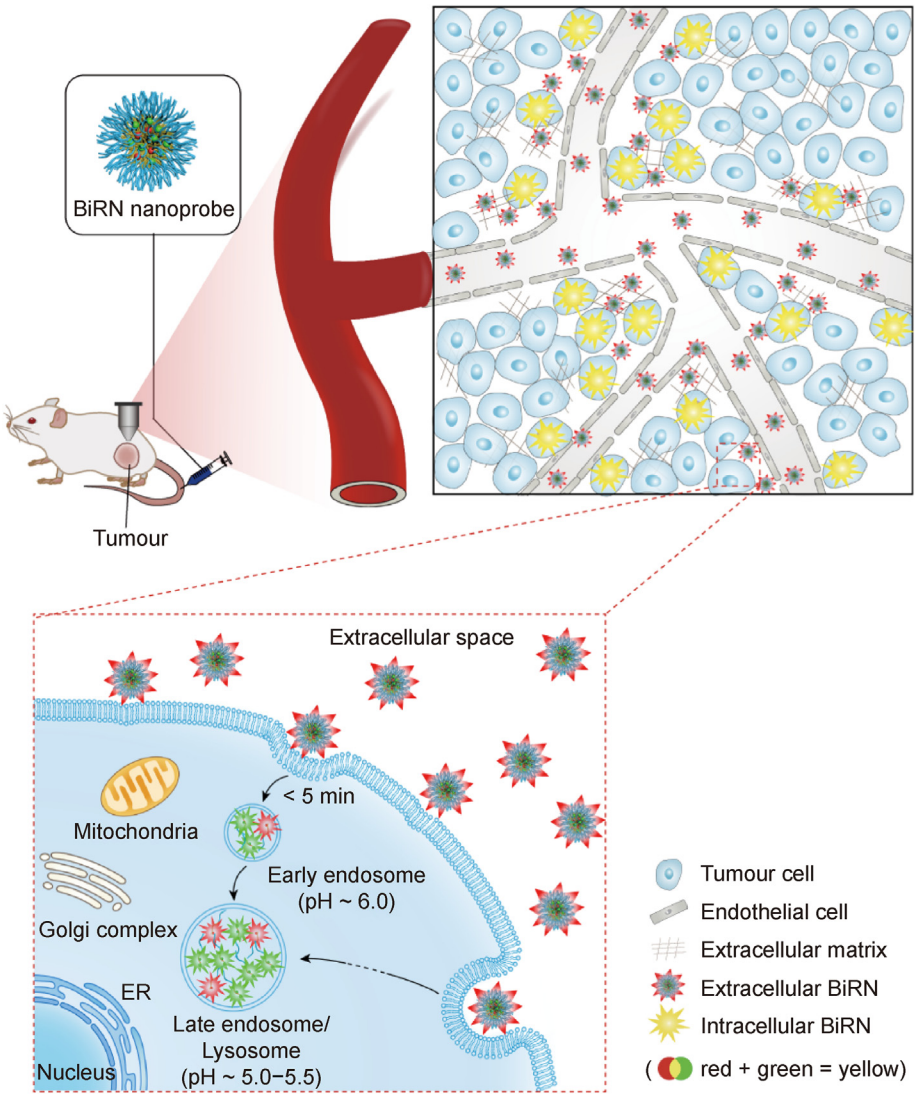

Fig. 4. The schematic representation of the internalization and activation processes of binary ratiometric nanoreporter (BiRN) nanoprobes in living mice. ER: endoplasmic reticulum. Reprinted from Ref. [91] with permission.

tumor tissues, the Cy5 signal of MRIN promptly turns 'ON' due to nanoparticle dissociation within the acidic endo-lysosomal environment (pH_{ee} ~ 6.0). In contrast, extracellularly distributed nanoparticles remain 'OFF', facilitating the measurement of internalized nanoparticles within tumor tissues. Subsequently, external 808 nm laser irradiation degrades the fluorescence quencher, effectively illuminating the Cy5 signals of extracellularly distributed nanoparticles in tumor tissues for precise quantification. Consequently, nanoparticles situated both intracellularly and extracellularly within tumor regions are selectively activated by non-crosstalk stimuli, allowing for monochromatic ratiometric imaging of nanoparticle microdistribution *in vivo*. Utilizing MRIN nanotechnology, this approach enables precise quantification of nanoparticle distribution within both extracellular and intracellular compartments across various tumor models.

The generation of FRET signals depends on the overlap between the donor emission spectrum and the acceptor absorption spectrum, as well as their appropriate spatial configuration, which ensures detection specificity. Despite significant advancements in FRET methodologies, challenges persist. FRET provides powerful qualitative analysis capabilities, but its quantitative analysis remains complex. Calculating FRET efficiency necessitates consideration of various factors, including spectral overlap between the donor and acceptor, fluorescence lifetime, and fluorescence quantum yield, all of which require intricate mathematical models and correction methods. Consequently, comprehensive pharmacokinetic analysis remains difficult to achieve. Furthermore, the bioactivity of fluorescent dyes can potentially influence the pharmacokinetic characteristics of Nano-DDSs. However, there is limited understanding of how the incorporation of fluorescent dye molecules into Nano-DDSs affects the pharmaceutical attributes of the cargo, such as chemical structure conformation, peptide folding, and nucleotide stability.

3.3.2. ACQ

ACQ is a phenomenon where highly emissive fluorophores, which are brightly fluorescent in dilute solutions, become weakly emissive or non-emissive upon aggregation [93,94]. In the context of nanocarrier imaging, ACQ probes emit fluorescence when they are molecularly dispersed within the nanocarrier matrix. However, this fluorescence is quenched upon their release into the surrounding aqueous environment. Consequently, the observed

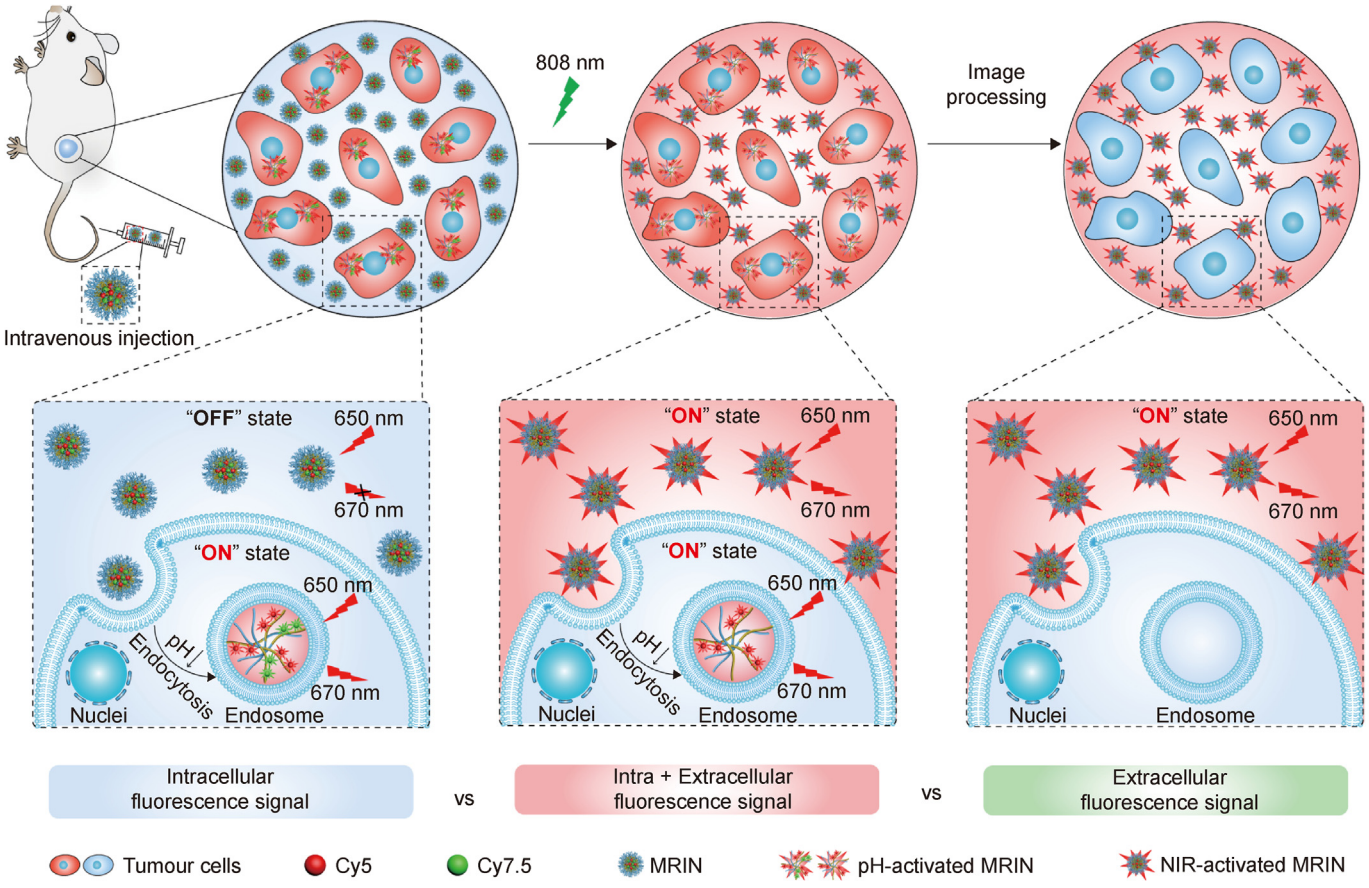

Fig. 5. Schematic representation of monochromatic ratiometric imaging for the quantification of extracellular and intracellular nanoparticle distribution in living mice. MRIN: monochromatic ratiometric imaging nanoparticle. Reprinted from Ref. [92] with permission.

fluorescence indicates the presence of intact nanocarriers (Fig. 3B). Utilizing ACQ, researchers have investigated the *in vivo* fates of various nanocarriers through live imaging techniques, yielding intriguing results that elucidate the significance of these nanocarriers [74].

In the study by He et al. [79], the biological fate of polymeric micelles following oral administration was investigated using near-infrared fluorophores with ACQ properties for labeling and tracking. The results provided valuable insights into the role of polymeric micelles in oral absorption. Similarly, Fan et al. [95] labeled monomethoxy poly(ethylene glycol)-poly(ε-caprolactone) (mPEG-PCL)-based nanocarriers with a near-infrared fluorophore exhibiting absolute ACQ properties, enabling precise bioimaging of nanoparticles. The study confirmed the relationship between fluorescence intensity and nanoparticle weight, facilitating the quantification of nanoparticles in blood, organs, and tissues. Despite the high density of PEG decoration, the nanocarriers demonstrated rapid clearance from the blood. Furthermore, pharmacokinetic profiles indicated faster clearance of the encapsulated drug compared to the nanocarriers. Fan et al. [96] employed an ACQ-based bioimaging strategy to study the pharmacokinetics and biodistribution of blank nanoemulsions, which mimic the formulation of Intralipid®. The information obtained is helpful for understanding the pharmacological and toxicological effects of nanoemulsions. Fu et al. [97] incorporated the ACQ probe P4 into SLNs and subsequently encapsulated them within integrating dissolving microneedles to investigate the transdermal diffusion of SLNs administered at various skin sites. The findings demonstrated that the stability of SLNs remained unaffected upon incorporation into integrating dissolving microneedles, as evidenced by the lack of significant alterations in fluorescence properties. Additionally, the study confirmed the site-specific nature of transdermal diffusion in nanocarrier-loaded SLNs.

ACQ is an important technique for monitoring the *in vivo* behavior of nanocarriers. In many biological assays, the ACQ effect can reduce background signals and enhance the signal-to-noise ratio of detection. However, ACQ-based biological imaging is not well-suited for hydrophilic nanocarriers. This limitation arises from the difficulty in encapsulating dyes within hydrophilic matrices and the rapid absorption of water molecules into these matrices, which leads to aggregation and premature fluorescence quenching. Since the ACQ effect depends on the degree of aggregation of fluorescent molecules, precise quantitative analysis becomes more complex. Furthermore, the *in vivo* release behavior of loaded ACQ probes may not fully align with that of the active pharmaceutical ingredient. The re-illumination caused by the disaggregation and redistribution of ACQ probe molecules into physiological hydrophobic regions may introduce potential interference, resulting in inaccurate analysis of the loaded drugs.

3.3.3. AIE

AIE-based fluorophores exhibit minimal fluorescence when existing as isolated molecules in a diluted state. However, upon aggregation or dispersion within nanoparticles, emission is induced due to the restriction of the free rotation of individual molecules [98]. Consequently, the encapsulated AIE probes illuminate the nanoparticles, while leaked probes produce minimal fluorescence [54,99] (Fig. 3C).

Chen et al. [100] utilized a combination of AIE and label-free mass spectrometry imaging to visualize and quantify AIE nanoparticles within tissue, while concurrently analyzing spatial metabolic changes. The findings suggested that the presence of nanoparticles in healthy tissues led to specific alterations in endogenous metabolism, including oxidative stress characterized by a reduction in glutathione levels. Furthermore, the limited efficacy of passive nanoparticle delivery to tumors suggested that the enhanced accumulation of nanoparticles in tumor tissues was not facilitated by the abundant presence of tumor vessels. In a study conducted by Wu et al. [101], a Pt(IV) prodrug activated by visible light and an AIE luminogen (AIEgen) were copolymerized and incorporated into the main chain of PtAIECP. Subsequently, doxorubicin (DOX) was encapsulated within nanoparticles formed by PtAIECP (PtAIECP@-DOX NP). The PtAIECP@DOX NP enabled the monitoring of both the activation of the Pt(IV) prodrug to Pt(II) and the release of DOX intracellularly through a fluorescence "turn-on" mechanism during visible-light-induced cleavage of the polymer main chain and dissociation of the self-assembled structure *in vitro* and *ex vivo*. This polyprodrug and AIE combination approach facilitated the simultaneous release and monitoring of two drugs. Zhang et al. [102] employed tetrakis (4-hydroxyphenyl) ethylene (THPE), an AIE fluorophore, as a representative compound to investigate the cellular uptake mechanisms and dissolution kinetics of nanocrystals within cells. Their findings, as revealed through confocal imaging and flow cytometry, indicate that nanocrystals can be internalized by cells either as intact nanoparticles or in their dissolved molecular form.

Since AIE probes produce almost no signal in solution, they can effectively reduce background noise and enhance the signal-to-noise ratio. However, while AIE probes emit strong fluorescence upon aggregation, this can also limit spatial resolution. In highly aggregated regions, excessively strong fluorescence signals may obscure subtle structural details, particularly in the study of subcellular structures. Additionally, in certain biological environments, non-specific adsorption can cause AIE probes to reaggregate, resulting in false fluorescent signals and compromising the accuracy of experimental results.

3.4. Mass spectrometry

Liquid chromatography/mass spectrometry (LC-MS) is a widely used technique for quantifying small molecular drugs and is increasingly employed for the quantification of constituent polymers in nanoparticles [35,47,53,103,104]. Polymers are characterized by their polydisperse molecular weights and their propensity to form multicharged ions in electrospray ionization mass spectrometry, resulting in a wide array of precursor ions. Conventional analytical techniques, such as the commonly used multiple reaction monitoring (MRM) scan mode, fail to provide a comprehensive profile necessary for the sensitive and accurate quantification of polymers *in vivo*. Zhou et al. [47] have developed a reliable method for the quantification of the most widely used polymeric nanomaterial, PEG, using liquid chromatography-quadrupole/time-of-flight mass spectrometry (LC-Q-TOF/MS), based on a full profile acquisition technique named MS^{ALL}. This technique employs information-independent acquisition, allowing all PEG precursor ions to pass through the first quadrupole into the collision cell, where collision-induced dissociation with appropriate collision energy effectively generates several common PEG-specific fragments, each consisting of a few ethylene oxide subunits, from all PEGs. Among these, a characteristic product ion is used to achieve highly sensitive, specific, and accurate absolute quantitation of PEGs with polydisperse molecular weights and numerous precursor ions. The major advantages of this technique include its capacity for comprehensive analysis of PEGs with excellent specificity, high sensitivity, and reproducibility. Compared to labeling methods, LC-Q-TOF/MS assays help to avoid artifacts from labels and reduce interference from degraded materials. Many researchers have developed LC-MS-based methods for the quantitative analysis and pharmacokinetic profiling of polymers in biological specimens [35,47,103–108].

Meng et al. [107] conducted an *in vivo* study on the amphiphilic diblock copolymer monomethoxy poly(ethylene glycol)-block-poly(d,L-lactic acid) (PEG-PLA) in rats, employing an LC-MS method for quantitative analysis based on the MS^{ALL} technique. This study investigated the pharmacokinetics, biodistribution, metabolism, and excretion of PEG-PLA following its intravenous administration in rats. The results indicated that unchanged PEG-PLA was primarily distributed to the spleen, liver, and kidneys, with subsequent elimination in urine over a 48-h period, predominantly (>80%) in the form of its PEG metabolite. Using a similar technique, Ren et al. [104] examined the pharmacokinetics, tissue distribution, and excretion of D-α-tocopheryl polyethylene glycol 1000 succinate (TPGS) and its metabolite, PEG1000, in rats following both oral and intravenous administration. Additionally, they investigated the interaction of TPGS with cytochromes P450 in human liver microsomes. Song et al. [109] studied the release kinetics of a novel trivalent PEGylated irinotecan (PEG-$[Irinotecan]_3$). The results demonstrated that PEG$[Irinotecan]_3$ underwent a gradual reduction in irinotecan content, resulting in the formation of PEG $[Irinotecan]_{3-x}$ (x = 2,1) and PEG-[linker], which led to the release of irinotecan and subsequent formation of the active compound SN-38. Šimek et al. [110] introduced a novel LC-MS methodology to evaluate the pharmacokinetic characteristics of free and encapsulated DOX within oleyl hyaluronan (HA-C18:1) polymeric micelles. Their findings revealed rapid dissociation of the nanocarriers following administration. Nevertheless, the encapsulated DOX demonstrated prolonged circulation time and improved tumor targeting.

3.5. Anti-PEG single-chain variable fragment antibody

Zhan's group [111] developed a facile method for separating PEGylated liposomal drugs using an anti-PEG single chain variable fragment antibody (PEG-scFv) in combination with high performance liquid chromatography to quantify released DOX and liposomal DOX in plasma. In this method, the PEG-scFv triggers the precipitation of PEGylated liposomes following incubation at a specific ratio. Validation has confirmed that the adsorption of PEG-scFv on these liposomes neither compromises their structural integrity nor leads to drug leakage. The precipitate can be easily separated from the released DOX in the supernatant through low-speed centrifugation (under 2,000 *g*). As a result, it becomes feasible to distinguish and measure both the liposomal DOX and the released DOX. This technique exhibited sufficient accuracy and sensitivity for assessing both released and encapsulated DOX. The same technique was employed for the separation of PEGylated polymeric micelles, resulting in successful separation under gentle centrifugation conditions unaffected by serum or plasma. This method was used to investigate the stability and *in vivo* performance of paclitaxel-loaded micelles, focusing on micelle-related complement activation and the pharmacokinetic profile [112]. In conclusion, the PEG-scFv method is deemed appropriate for the thorough separation of PEGylated liposomes and polymeric micelles, as well as potentially other PEGylated nanocarriers.

3.6. Other techniques

Wang et al. [38] developed a method combining solid-phase extraction with LC-MS to detect both encapsulated and released

DOX in PEGylated DOX liposomes. The poor retention of PEGylated DOX liposomes and the strong retention of released DOX on reversed-phase solid-phase extraction columns enabled the separation of encapsulated DOX from tissue samples. Subsequently, the concentrations of encapsulated DOX and total DOX are measured separately by LC-MS, with the concentration of released DOX determined by the difference between these two values. The study compared the release and uptake profiles of DOX in PEGylated liposomes between normal tissues and tumor tissues in tumor-bearing mice. The results demonstrated that liposomes effectively released DOX into tumors, enhancing tumor uptake of DOX by 1.8-fold compared to direct administration of a DOX solution. Additionally, liposomes reduced DOX distribution to the heart, thereby decreasing its cardiac toxicity.

Dialysis is frequently employed to investigate the *in vitro* drug release behavior of nanomedicines, serving as a surrogate for *in vivo* drug release studies. Sethi et al. [113] investigated the release profile of 5-fluorouracil encapsulated within cross-linked chitosan nanoparticles in phosphate-buffered saline (PBS) at pH 7.4. Ma et al. [114] evaluated the drug release kinetics of cyclodextrin-modified PLGA nanoparticles using a reverse dialysis method in PBS at pH values of 7.4, 6.8, and 5.0. However, it is important to note that *in vitro* buffer systems cannot fully replicate the physiological conditions of blood flow, plasma proteins, and cellular components present *in vivo*. Consequently, *in vitro* drug release assays may not accurately represent the actual release behavior of nanoparticles within the bloodstream. Furthermore, drug adsorption by the dialysis membrane can also introduce significant inaccuracies in the results.

4. Conclusion and perspectives

The precise timing, location, and mechanism of drug release from nanocarriers, as well as the interactions between nanocarriers, nanomaterials, and body, remain largely unknown. Without a comprehensive understanding of *in vivo* processes, accurately predicting the efficacy and potential toxicity of Nano-DDSs is challenging. Relying solely on feedback from terminal biological effects to inform the optimization of Nano-DDSs renders their development speculative and inefficient in terms of research and development resources. Given the dynamic processes involving released drugs, encapsulated drugs, and nanomaterials in Nano-DDSs, identifying suitable monitoring techniques to track *in vivo* changes is paramount for advancing the clinical translation of nanomedicines. This review provides an overview of current bioanalytical techniques used to assess the pharmacokinetics of Nano-DDSs. However, there remains a pressing need to develop more effective bioanalytical methods that enable precise analysis of the multiple components of Nano-DDSs *in vivo*.

As research on the *in vivo* fate of nanomedicines advances, it becomes crucial to study the interactions between nanomedicines and various cell types, including tumor cells, immune cells, and endothelial cells. Analyzing the distribution and trajectories of nanomedicines within cells, and exploring the interactions between nanomedicines and biomacromolecules, will enhance our understanding of how nanomedicines interact with the biological systems. To achieve these objectives, it is necessary to overcome technical challenges and develop more efficient, sensitive, and precise analytical techniques. This will enable a more comprehensive and in-depth elucidation of the *in vivo* fate of Nano-DDSs, facilitating the effective design and optimization of nanomedicines. Furthermore, traditional pharmacokinetic modeling is inadequate for characterizing the pharmacokinetic behavior of nanomedicines. There is a need to establish novel pharmacokinetic models that consider the dynamic equilibrium between the released and encapsulated forms of the drug, the nanocarrier's stability within the body, its interactions with plasma proteins and particular organs, and any metabolic processes the nanocarrier undergoes *in vivo*.

CRediT authorship contribution statement

Xiangjun Meng: Writing – review & editing, Writing – original draft, Funding acquisition, Conceptualization. **Jiayi Yao:** Software, Investigation. **Jingkai Gu:** Writing – review & editing, Supervision, Funding acquisition.

Declaration of competing interest

As an editorial board member, Jingkai Gu recused himself from all review processes related to this article to ensure the fairness and objectivity of the review. Other authors declare that there are no conflicts of interest.

Acknowledgments

This work was supported by the National Natural Science Foundation of China (Grant Nos.: 82304443, 82030107, and 82373944).

References

[1] M.E.R. O'Brien, N. Wigler, M. Inbar, et al., Reduced cardiotoxicity and comparable efficacy in a phase III trial of pegylated liposomal doxorubicin HCl (CAELYX/Doxil) versus conventional doxorubicin for first-line treatment of metastatic breast cancer, Ann. Oncol. 15 (2004) 440–449.
[2] D.W. Northfelt, B.J. Dezube, J.A. Thommes, et al., Pegylated-liposomal doxorubicin versus doxorubicin, bleomycin, and vincristine in the treatment of AIDS-related Kaposi's sarcoma: Results of a randomized phase III clinical trial, J. Clin. Oncol. 16 (1998) 2445–2451.
[3] G. Batist, J. Barton, P. Chaikin, et al., Myocet (liposome-encapsulated doxorubicin citrate): A new approach in breast cancer therapy, Expert Opin. Pharmacother. 3 (2002) 1739–1751.
[4] E. Rosenthal, I. Poizot-Martin, T. Saint-Marc, et al., Phase IV study of liposomal daunorubicin (DaunoXome) in AIDS-related Kaposi sarcoma, Am. J. Clin. Oncol. 25 (2002) 57–59.
[5] S. Koudelka, J. Turánek, Liposomal paclitaxel formulations, J. Control. Release 163 (2012) 322–334.
[6] F. Jahn, K. Jordan, T. Behlendorf, et al., Safety and efficacy of liposomal cytarabine in the treatment of neoplastic meningitis, Oncology 89 (2015) 137–142.
[7] J.E. Frampton, Mifamurtide: A review of its use in the treatment of osteosarcoma, Paediatr, Drugs 12 (2010) 141–153.
[8] FDA approves liposomal vincristine (Marqibo) for rare leukemia, Oncology (Williston Park) 26 (2012), 841.
[9] A. Wang-Gillam, C.P. Li, G. Bodoky, et al., Nanoliposomal irinotecan with fluorouracil and folinic acid in metastatic pancreatic cancer after previous gemcitabine-based therapy (NAPOLI-1): A global, randomised, open-label, phase 3 trial, Lancet 387 (2016) 545–557.
[10] N. Heldring, H. Bjermo, A. Brize, et al., Nanoparticle micellar formulation of paclitaxel in combination with carboplatin for women with recurrent platinum sensitive ovarian cancer (OAS07-OVA): Overall survival results of a phase 3 randomized trial, J. Clin. Oncol. 36 (2018), 5560.
[11] W.J. Gradishar, S. Tjulandin, N. Davidson, et al., Phase III trial of nanoparticle albumin-bound paclitaxel compared with polyethylated castor oil-based paclitaxel in women with breast cancer, J. Clin. Oncol. 23 (2005) 7794–7803.
[12] T. Saeki, H. Mukai, J. Ro, et al., A global phase III clinical study comparing NK105 and paclitaxel in metastatic or recurrent breast cancer patients, Ann. Oncol. 28 (2017) v80–v81.
[13] M.M. Jain, S.U. Gupte, S.G. Patil, et al., Paclitaxel injection concentrate for nanodispersion versus nab-paclitaxel in women with metastatic breast cancer: A multicenter, randomized, comparative phase II/III study, Breast Cancer Res. Treat. 156 (2016) 125–134.
[14] H. He, L. Liu, E.E. Morin, et al., Survey of clinical translation of cancer nanomedicines-lessons learned from successes and failures, Acc. Chem. Res. 52 (2019) 2445–2461.
[15] S. Wilhelm, A.J. Tavares, Q. Dai, et al., Analysis of nanoparticle delivery to tumours, Nat. Rev. Mater. 1 (2016), 16014.
[16] K.T. Schmidt, F. Karzai, M. Bilusic, et al., A single-arm phase II study combining NLG207, a nanoparticle camptothecin, with enzalutamide in advanced metastatic castration-resistant prostate cancer post-enzalutamide, Oncologist 27 (2022) 718–e694.

[17] Merrimack Discontinues Development of MM-310. http://investors.merrimack.com/news-releases/news-release-details/merrimack-discontinues-development-mm-310. (Accessed 10 July 2024).
[18] J. Lazarovits, Y.Y. Chen, E.A. Sykes, et al., Nanoparticle-blood interactions: The implications on solid tumour targeting, Chem. Commun. (Camb.) 51 (2015) 2756–2767.
[19] X. Sun, G. Wang, H. Zhang, et al., The blood clearance kinetics and pathway of polymeric micelles in cancer drug delivery, ACS Nano 12 (2018) 6179–6192.
[20] K.M. Tsoi, S.A. MacParland, X.Z. Ma, et al., Mechanism of hard-nanomaterial clearance by the liver, Nat. Mater. 15 (2016) 1212–1221.
[21] Y.N. Zhang, W. Poon, A.J. Tavares, et al., Nanoparticle-liver interactions: Cellular uptake and hepatobiliary elimination, J. Control. Release 240 (2016) 332–348.
[22] Q. Dai, C. Walkey, W.C.W. Chan, Polyethylene glycol backfilling mitigates the negative impact of the protein corona on nanoparticle cell targeting, Angew. Chem. Int. Ed. Engl. 53 (2014) 5093–5096.
[23] M. Ichihara, T. Shimizu, A. Imoto, et al., Anti-PEG IgM response against PEGylated liposomes in mice and rats, Pharmaceutics 3 (2010) 1–11.
[24] M. Hashida, Role of pharmacokinetic consideration for the development of drug delivery systems: A historical overview, Adv. Drug Deliv. Rev. 157 (2020) 71–82.
[25] N. Feliu, W.J. Parak, Developing future nanomedicines, Science 384 (2024) 385–386.
[26] L. Yuan, Q. Chen, J.E. Riviere, et al., Pharmacokinetics and tumor delivery of nanoparticles, J. Drug Deliv. Sci. Technol. 83 (2023), 104404.
[27] X. Shao, C. Shi, S. Wu, et al., Review of the pharmacokinetics of nanodrugs, Nanotechnol. Rev. 12 (2023), 20220525.
[28] X. Cai, M. Jin, L. Yao, et al., Physicochemical properties, pharmacokinetics, toxicology and application of nanocarriers, J. Mater. Chem. B 11 (2023) 716–733.
[29] M. Sarkar, Y. Wang, O. Ekpenyong, et al., Pharmacokinetic behaviors of soft nanoparticulate formulations of chemotherapeutics, Wiley Interdiscip. Rev. Nanomed. Nanobiotechnol. 15 (2023), e1846.
[30] M. Ghezzi, S. Pescina, C. Padula, et al., Polymeric micelles in drug delivery: An insight of the techniques for their characterization and assessment in biorelevant conditions, J. Control. Release 332 (2021) 312–336.
[31] N. Kaeokhamloed, S. Legeay, E. Roger, FRET as the tool for *in vivo* nanomedicine tracking, J. Control. Release 349 (2022) 156–173.
[32] D. Sun, S. Zhou, W. Gao, What went wrong with anticancer nanomedicine design and how to make it right, ACS Nano 14 (2020) 12281–12290.
[33] V. Agrahari, V. Agrahari, Facilitating the translation of nanomedicines to a clinical product: Challenges and opportunities, Drug Discov. Today 23 (2018) 974–991.
[34] L. Li, T. Yi, C.W. Lam, Interactions between human multidrug resistance related protein (MRP2; ABCC2) and excipients commonly used in self-emulsifying drug delivery systems (SEDDS), Int. J. Pharm. 447 (2013) 192–198.
[35] T. Wang, Y. Guo, Y. He, et al., Impact of molecular weight on the mechanism of cellular uptake of polyethylene glycols (PEGs) with particular reference to P-glycoprotein, Acta Pharm. Sin. B 10 (2020) 2002–2009.
[36] Q. Shen, Y. Lin, T. Handa, et al., Modulation of intestinal P-glycoprotein function by polyethylene glycols and their derivatives by *in vitro* transport and *in situ* absorption studies, Int. J. Pharm. 313 (2006) 49–56.
[37] C.B. Rodell, P. Baldwin, B. Fernandez, et al., Quantification of cellular drug biodistribution addresses challenges in evaluating *in vitro* and *in vivo* encapsulated drug delivery, Adv. Ther. 4 (2021), 2000125.
[38] H. Wang, M. Zheng, J. Gao, et al., Uptake and release profiles of PEGylated liposomal doxorubicin nanoparticles: A comprehensive picture based on separate determination of encapsulated and total drug concentrations in tissues of tumor-bearing mice, Talanta 208 (2020), 120358.
[39] L.S.L. Price, S.T. Stern, A.M. Deal, et al., A reanalysis of nanoparticle tumor delivery using classical pharmacokinetic metrics, Sci. Adv. 6 (2020), eaay9249.
[40] K. Greish, A. Mathur, M. Bakhiet, et al., Nanomedicine: Is it lost in translation? Ther. Deliv. 9 (2018) 269–285.
[41] H.L. Jang, Y.S. Zhang, A. Khademhosseini, Boosting clinical translation of nanomedicine, Nanomedicine (Lond) 11 (2016) 1495–1497.
[42] J. Hrkach, D. von Hoff, M. Mukkaram Ali, et al., Preclinical development and clinical translation of a PSMA-targeted docetaxel nanoparticle with a differentiated pharmacological profile, Sci. Transl. Med. 4 (2012), 128ra39.
[43] A. Dikpati, N. Gaudreault, V. Chénard, et al., Size Exclusion of Radioactive Polymers (SERP) informs on the biodegradation of trimethyl chitosan and biodegradable polymer nanoparticles *in vitro* and *in vivo*, J. Control. Release 346 (2022) 20–31.
[44] J.W. Nichols, Y.H. Bae, Odyssey of a cancer nanoparticle: From injection site to site of action, Nano Today 7 (2012) 606–618.
[45] R.K. Jain, T. Stylianopoulos, Delivering nanomedicine to solid tumors, Nat. Rev. Clin. Oncol. 7 (2010) 653–664.
[46] A.T. Florence, "Targeting" nanoparticles: The constraints of physical laws and physical barriers, J. Control. Release 164 (2012) 115–124.
[47] X. Zhou, X. Meng, L. Cheng, et al., Development and application of an MS^{ALL}-based approach for the quantitative analysis of linear polyethylene glycols in rat plasma by liquid chromatography triple-quadrupole/time-of-flight mass spectrometry, Anal. Chem. 89 (2017) 5193–5200.
[48] Z. Zhang, H. Jiang, Y. Zhang, et al., Comprehensive bioanalysis of ultrahigh molecular weight, highly disperse Poly(ethylene oxide) in rat *via* microsolid phase extraction and RPLC-Q-Q-TOF coupled with the MS^{ALL} technique, Anal. Chem. 92 (2020) 5978–5985.
[49] V. Lebreton, S. Legeay, P. Saulnier, et al., Specificity of pharmacokinetic modeling of nanomedicines, Drug Discov. Today 26 (2021) 2259–2268.
[50] S. Bonnet, R. Elfatairi, F. Franconi, et al., Organic nanoparticle tracking during pharmacokinetic studies, Nanomedicine (Lond) 16 (2021) 2539–2536.
[51] M. Germain, F. Caputo, S. Metcalfe, et al., Delivering the power of nanomedicine to patients today, J. Control. Release 326 (2020) 164–171.
[52] W. Wu, T. Li, Unraveling the *in vivo* fate and cellular pharmacokinetics of drug nanocarriers, Adv. Drug Deliv. Rev. 143 (2019) 1–2.
[53] T. Wang, D. Zhang, D. Sun, et al., Current status of *in vivo* bioanalysis of nano drug delivery systems, J. Pharm. Anal. 10 (2020) 221–232.
[54] Y. Cai, J. Qi, Y. Lu, et al., The *in vivo* fate of polymeric micelles, Adv. Drug Deliv. Rev. 188 (2022), 114463.
[55] K. Nigam, A. Kaur, A. Tyagi, et al., Baclofen-loaded poly (D, L-lactide-co-glycolic acid) nanoparticles for neuropathic pain management: *in vitro* and *in vivo* evaluation, Rejuvenation Res 22 (2019) 235–245.
[56] L. Mondal, B. Mukherjee, K. Das, et al., CD-340 functionalized doxorubicin-loaded nanoparticle induces apoptosis and reduces tumor volume along with drug-related cardiotoxicity in mice, Int. J. Nanomedicine 14 (2019) 8073–8094.
[57] T.L. Braga, S.R. Pinto, S.R.R. Dos Reis, et al., Octreotide nanoparticles showed affinity for *in vivo* MIA paca-2 inducted pancreas ductal adenocarcinoma mimicking pancreatic polypeptide-secreting tumor of the distal pancreas (PPoma), Pharm. Res. 36 (2019), 143.
[58] X. Zhong, K. Yang, Z. Dong, et al., Polydopamine as a biocompatible multifunctional nanocarrier for combined radioisotope therapy and chemotherapy of cancer, Adv. Funct. Mater. 25 (2015) 7327–7336.
[59] P. Areses, M.T. Agüeros, G. Quincoces, et al., Molecular imaging techniques to study the biodistribution of orally administered ^{99m}Tc-labelled naive and ligand-tagged nanoparticles, Mol. Imaging Biol. 13 (2011) 1215–1223.
[60] S.R.R. do Reis, E. Helal-Neto, A.O. da Silva de Barros, et al., Dual encapsulated dacarbazine and zinc phthalocyanine polymeric nanoparticle for photodynamic therapy of melanoma, Pharm. Res. 38 (2021) 335–346.
[61] I. Rather, N. Shafiq, J. Shukla, et al., Bio-evaluation of poly(lactic-co-glycolic) acid nanoparticles loaded with radiolabelled rifampicin, Br. J. Clin. Pharmacol. 89 (2023) 3702–3714.
[62] I.H.C. Miedema, G.J.C. Zwezerijnen, M.C. Huisman, et al., PET-CT imaging of polymeric nanoparticle tumor accumulation in patients, Adv. Mater. 34 (2022), e2201043.
[63] X. Wang, G. Rong, J. Yan, et al., *In vivo* tracking of fluorinated polypeptide gene carriers by positron emission tomography imaging, ACS Appl. Mater. Interfaces 12 (2020) 45763–45771.
[64] S. Nagachinta, G. Becker, S. Dammicco, et al., Radiolabelling of lipid-based nanocarriers with fluorine-18 for *in vivo* tracking by PET, Colloids Surf. B Biointerfaces 188 (2020), 110793.
[65] H. Wang, P. Guo, Radiolabeled RNA nanoparticles for highly specific targeting and efficient tumor accumulation with favorable *in vivo* biodistribution, Mol. Pharm. 18 (2021) 2924–2934.
[66] J. Pellico, P.J. Gawne, R.T.M. de Rosales, Radiolabelling of nanomaterials for medical imaging and therapy, Chem. Soc. Rev. 50 (2021) 3355–3423.
[67] S.L. Skoczen, S.T. Stern, Improved ultrafiltration method to measure drug release from nanomedicines utilizing a stable isotope tracer, Methods Mol. Biol. 1682 (2018) 223–239.
[68] S. Skoczen, S.E. McNeil, S.T. Stern, Stable isotope method to measure drug release from nanomedicines, J. Control. Release 220 (2015) 169–174.
[69] S.L. Skoczen, K.S. Snapp, R.M. Crist, et al., Distinguishing pharmacokinetics of marketed nanomedicine formulations using a stable isotope tracer assay, ACS Pharmacol. Transl. Sci. 3 (2020) 547–558.
[70] D. Hwang, N. Vinod, S.L. Skoczen, et al., Bioequivalence assessment of high-capacity polymeric micelle nanoformulation of paclitaxel and Abraxane® in rodent and non-human primate models using a stable isotope tracer assay, Biomaterials 278 (2021), 121140.
[71] K. Li, B. Liu, Polymer-encapsulated organic nanoparticles for fluorescence and photoacoustic imaging, Chem. Soc. Rev. 43 (2014) 6570–6597.
[72] G. Yang, Y. Liu, C.X. Zhao, Quantitative comparison of different fluorescent dye-loaded nanoparticles, Colloids Surf. B Biointerfaces 206 (2021), 111923.
[73] G. Yang, Y. Liu, J. Teng, et al., FRET ratiometric nanoprobes for nanoparticle monitoring, Biosensors 11 (2021), 505.
[74] J. Qi, X. Hu, X. Dong, et al., Towards more accurate bioimaging of drug nanocarriers: Turning aggregation-caused quenching into a useful tool, Adv. Drug Deliv. Rev. 143 (2019) 206–225.
[75] S. Mannucci, F. Boschi, B. Cisterna, et al., A correlative imaging study of *in vivo* and *ex vivo* biodistribution of solid lipid nanoparticles, Int. J. Nanomedicine 15 (2020) 1745–1758.
[76] G. Zhang, Y. Wang, Z. Zhang, et al., FRET imaging revealed that nanocrystals enhanced drug oral absorption by dissolution rather than endocytosis: A case study of coumarin 6, J. Control. Release 332 (2021) 225–232.
[77] Tengjisi, Y. Liu, D. Zou, et al., Bioinspired core-shell silica nanoparticles monitoring extra- and intra-cellular drug release, J. Colloid Interface Sci. 624 (2022) 242–250.
[78] J. Zhong, Y. Quan, X. Zhao, et al., Coassembling functionalized glycopolypeptides to prepare pH-responsive self-indicating nano complexes to manipulate self-assembly/drug delivery and visualize intracellular drug release, Biomater Adv. 134 (2022), 112711.

[79] H. He, L. Wang, Y. Ma, et al., The biological fate of orally administered mPEG-PDLLA polymeric micelles, J. Control. Release 327 (2020) 725–736.
[80] Y. Jiang, Y. Jiang, Z. Ding, et al., Investigation of the "nose-to-brain" pathways in intranasal HupA nanoemulsions and evaluation of their *in vivo* pharmacokinetics and brain-targeting ability, Int. J. Nanomed. 17 (2022) 3443–3456.
[81] Y. Xu, N. Liang, J. Liu, et al., Design and fabrication of chitosan-based AIE active micelles for bioimaging and intelligent delivery of paclitaxel, Carbohydr. Polym. 290 (2022), 119509.
[82] C. Sun, J. Lu, J. Wang, et al., Redox-sensitive polymeric micelles with aggregation-induced emission for bioimaging and delivery of anticancer drugs, J. Nanobiotechnol. 19 (2021), 14.
[83] R. Wang, L. Zou, Z. Yi, et al., PLGA nanoparticles loaded with curcumin produced luminescence for cell bioimaging, Int. J. Pharm. 639 (2023), 122944.
[84] E.A. Jares-Erijman, T.M. Jovin, FRET imaging, Nat. Biotechnol. 21 (2003) 1387–1395.
[85] V. Lebreton, N. Kaeokhamloed, A. Vasylaki, et al., Pharmacokinetics of intact lipid nanocapsules using new quantitative FRET technique, J. Control. Release 351 (2022) 681–691.
[86] A.S. Klymchenko, F. Liu, M. Collot, et al., Dye-loaded nanoemulsions: Biomimetic fluorescent nanocarriers for bioimaging and nanomedicine, Adv. Healthc. Mater. 10 (2021), e2001289.
[87] V. Marx, Probes: FRET sensor design and optimization, Nat. Meth. 14 (2017) 949–953.
[88] C. Zhu, L. Luo, X. Jiang, et al., Selective intratumoral drug release and simultaneous inhibition of oxidative stress by a highly reductive nanosystem and its application as an anti-tumor agent, Theranostics 10 (2020) 1166–1180.
[89] L. Sun, J. Zhang, J.E. Zhou, et al., Monitoring the *in vivo* siRNA release from lipid nanoparticles based on the fluorescence resonance energy transfer principle, Asian J. Pharm. Sci. 18 (2023), 100769.
[90] S. Datta, V. Huntošová, A. Jutková, et al., Influence of hydrophobic side-chain length in amphiphilic gradient copoly(2-oxazoline)s on the therapeutics loading, stability, cellular uptake and pharmacokinetics of nano-formulation with curcumin, Pharmaceutics 14 (2022), 2576.
[91] Q. Yin, A. Pan, B. Chen, et al., Quantitative imaging of intracellular nanoparticle exposure enables prediction of nanotherapeutic efficacy, Nat. Commun. 12 (2021), 2385.
[92] Y. Yan, B. Chen, Q. Yin, et al., Dissecting extracellular and intracellular distribution of nanoparticles and their contribution to therapeutic response by monochromatic ratiometric imaging, Nat. Commun. 13 (2022), 2004.
[93] X. Ma, R. Sun, J. Cheng, et al., Fluorescence aggregation-caused quenching versus aggregation-induced emission: A visual teaching technology for undergraduate chemistry students, J. Chem. Educ. 93 (2016) 345–350.
[94] N. Zhao, J.W. Lam, H.H. Sung, et al., Effect of the counterion on light emission: A displacement strategy to change the emission behaviour from aggregation-caused quenching to aggregation-induced emission and to construct sensitive fluorescent sensors for Hg^{2+} detection, Chemistry 20 (2014) 133–138.
[95] W. Fan, H. Peng, Z. Yu, et al., The long-circulating effect of pegylated nanoparticles revisited via simultaneous monitoring of both the drug payloads and nanocarriers, Acta Pharm. Sin. B 12 (2022) 2479–2493.
[96] W. Fan, Z. Yu, H. Peng, et al., Effect of particle size on the pharmacokinetics and biodistribution of parenteral nanoemulsions, Int. J. Pharm. 586 (2020), 119551.
[97] Y. Fu, C. Shi, X. Li, et al., Demonstrating biological fate of nanoparticle-loaded dissolving microneedles with aggregation-caused quenching probes: Influence of application sites, Pharmaceutics 15 (2023), 169.
[98] L. Yan, Y. Zhang, B. Xu, et al., Fluorescent nanoparticles based on AIE fluorogens for bioimaging, Nanoscale 8 (2016) 2471–2487.
[99] H. Wang, G. Liu, Advances in luminescent materials with aggregation-induced emission (AIE) properties for biomedical applications, J. Mater. Chem. B 6 (2018) 4029–4042.
[100] J. Chen, L. Mao, Y. Jiang, et al., Revealing the *in situ* behavior of aggregation-induced emission nanoparticles and their biometabolic effects via mass spectrometry imaging, ACS Nano 17 (2023) 4463–4473.
[101] P. Wu, X. Wang, Z. Wang, et al., Light-activatable prodrug and AIEgen copolymer nanoparticle for dual-drug monitoring and combination therapy, ACS Appl. Mater. Interfaces 11 (2019) 18691–18700.
[102] J. Zhang, C.D. Corpstein, T. Li, Intracellular uptake of nanocrystals: Probing with aggregation-induced emission of fluorescence and kinetic modeling, Acta Pharm. Sin. B 11 (2021) 1021–1029.
[103] L. Yin, T. Ren, S. Zhao, et al., Comparative pharmacokinetic study of PEGylated gemcitabine and gemcitabine in rats by LC-MS/MS coupled with pre-column derivatization and MS^{ALL} technique, Talanta 206 (2020), 120184.
[104] T. Ren, R. Li, L. Zhao, et al., Biological fate and interaction with cytochromes P450 of the nanocarrier material, d-α-tocopheryl polyethylene glycol 1000 succinate, Acta Pharm. Sin. B 12 (2022) 3156–3166.
[105] M. Shi, X. Zheng, H. Jiang, et al., Unraveling the *in vivo* biological fate of mPEG2000-PDLLA2500-COOH diblock copolymers by LC-MS/MS based on CID in source technique, Anal. Chim. Acta 1267 (2023), 341375.
[106] M. Shi, H. Jiang, L. Yin, et al., Development of an UPLC-MS/MS method coupled with in-source CID for quantitative analysis of PEG-PLA copolymer and its application to a pharmacokinetic study in rats, J. Chromatogr. B Analyt. Technol. Biomed. Life. Sci. 1125 (2019), 121716.
[107] X. Meng, Z. Zhang, J. Tong, et al., The biological fate of the polymer nanocarrier material monomethoxy poly(ethylene glycol)-*block*-poly(d, l-lactic acid) in rat, Acta Pharm. Sin. B 11 (2021) 1003–1009.
[108] R. Bai, D. Sun, Y. Shan, et al., Disposition and fate of polyoxyethylene glycerol ricinoleate as determined by LC-Q-TOF MS coupled with MS^{ALL}, SWATH and HR MS/MS techniques, Chin. Chem. Lett. 32 (2021) 3237–3240.
[109] S. Song, D. Sun, H. Wang, et al., Full-profile pharmacokinetics, anticancer activity and toxicity of an extended release trivalent PEGylated irinotecan prodrug, Acta Pharm. Sin. B 13 (2023) 3444–3453.
[110] M. Šimek, M. Hermannová, D. Šmejkalová, et al., LC-MS/MS study of *in vivo* fate of hyaluronan polymeric micelles carrying doxorubicin, Carbohydr. Polym. 209 (2019) 181–189.
[111] W. Tang, Z. Zhang, C. Li, et al., Facile separation of PEGylated liposomes enabled by anti-PEG scFv, Nano Lett. 21 (2021) 10107–10113.
[112] S. Lin, Y. Yu, E. Wu, et al., Reexamining *in vivo* fate of paclitaxel-loaded polymeric micelles, Nano Today 56 (2024), 102255.
[113] A. Sethi, M. Ahmad, T. Huma, et al., Evaluation of low molecular weight cross linked chitosan nanoparticles, to enhance the bioavailability of 5-flourouracil, Dose-response 19 (2021), 15593258211025353.
[114] P. Ma, J. Huang, J. Liu, et al., Nanoformulation of paclitaxel: Exploring the cyclodextrin/PLGA nano delivery carrier to slow down paclitaxel release, enhance accumulation *in vivo*, J. Cancer 14 (2023) 759–769.